ACS Macro Letters

Letter

pubs.acs.org/macroletters

Block Copolymer Nanocomposites in Electric Fields: Kinetics of Alignment

Clemens Liedel,[†] Christian W. Pester,[†] Markus Ruppel,[‡] Christian Lewin,[†] Mariela J. Pavan,[§] Volker S. Urban,[∥] Roy Shenhar,[§] Peter Bösecke,[⊥] and Alexander Böker*[,†,#]

[†]Macromolecular Materials and Surfaces, RWTH Aachen University and DWI an der RWTH Aachen e.V., Forckenbeckstraße 50, 52056 Aachen, Germany

[‡]Chemical Sciences Division, Oak Ridge National Laboratory (ORNL), Oak Ridge, Tennessee 37831, United States

[§]Institute of Chemistry, and the Center for Nanoscience and Nanotechnology, The Hebrew University of Jerusalem, Jerusalem, 91904, Israel

[∥]Biology and Soft Matter Division, Oak Ridge National Laboratory (ORNL), Oak Ridge, Tennessee 37831, United States

[⊥]European Synchrotron Radiation Facility (ESRF), 6 rue Jules Horowitz, 38043 Grenoble Cedex, France

[#]JARA-FIT, RWTH Aachen University, 52056 Aachen, Germany

S *Supporting Information*

ABSTRACT: We investigate the kinetics of block copolymer/nanoparticle composite alignment in an electric field using in situ transmission small-angle X-ray scattering. As a model system, we employ a lamellae forming polystyrene-*block*-poly(2-vinyl pyridine) block copolymer with different contents of gold nanoparticles in thick films under solvent vapor annealing. While the alignment improves with increasing nanoparticle fraction, the kinetics slows down. This is explained by changes in the degree of phase separation and viscosity. Our findings provide extended insights into the basics of nanocomposite alignment.

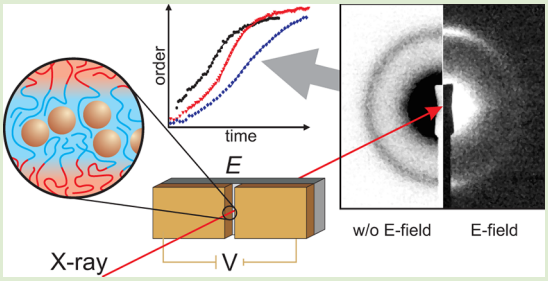

Block copolymers spontaneously phase separate with domain spacings in the range of 5 to 100 nm.[1] Because of this mesoscopic size, they are potentially suited for downscaling electronic devices.[2,3] Still, without further treatment, ordered domains in phase-separated block copolymer films only cover areas of a few micrometers or less in diameter. To overcome this drawback, several methods to align block copolymers in thin films have been introduced. Besides mechanical methods,[4−8] guided solvent evaporation,[9,10] temperature gradients,[11] and templated self-assembly,[12−15] magnetic[16−20] or electric fields can be used.[21−29] The latter permit local control over domain orientation, and the effects even on single defects can be studied.[25,26,28]

Selective incorporation of metallic nanoparticles in block copolymers is gaining increasing attention recently,[30−37] as it greatly improves the utilization of nanoparticles in various devices. Besides enhancing the mechanical strength, catalytic activity, optical and magnetic properties,[38] nanoparticles in block copolymers have been shown to improve the dielectric contrast[39,40] and conductivity.[41] By combining alignment of block copolymers in electric fields with dispersing nanoparticles in block copolymers, we recently demonstrated the possibility of manufacturing one-dimensionally aligned nanoparticle structures.[42] For producing arrays of aligned metallic structures, this is a promising alternative to the utilization of block copolymers as lithographic masks[43−45] or as templates for selective reduction of metal precursors.[46−48] For further applications, however, understanding the kinetics of block copolymer/nanoparticle composite alignment in electric fields is of key importance.

Block copolymer alignment in electric fields has been extensively studied using scattering methods in polymer films,[23,24,49−57] bulk material, and concentrated solutions,[21,58−64] and insights on the alignment kinetics were gained. However, real alignment kinetics during in-plane alignment in polymer films has not been investigated. Recently, first measurements have been devised using a quasi in situ atomic force microscopy (AFM) technique.[25,26] However, because the field had to be switched off for each image acquisition, no exact kinetic information was accessible. Thus, there is the need for a different experimental setup, which we describe in the present paper.

We present the alignment kinetics of a polystyrene-*block*-poly(2-vinyl pyridine) (PS-*b*-P2VP) block copolymer under solvent vapor annealing during application of an in-plane DC electric field. Further, we discuss the influence of gold nanoparticles dispersed in this diblock on the kinetics of alignment in a DC electric field during toluene vapor annealing.

Received: October 2, 2012
Accepted: December 19, 2012
Published: December 26, 2012

   dx.doi.org/10.1021/mz3005132 | *ACS Macro Lett.* 2013, 2, 53−58

After a brief discussion of the experimental method and evaluation, we present SAXS patterns and AFM images of polymer films before and after annealing in the presence of an electric field. Further, we describe and analyze the change in the order parameter with time that we calculate from in situ SAXS experiments.

Figure 1 shows the setup of our SAXS experiments at ID2, ESRF, France. The order parameter P_2 quantifies the degree of orientational order with respect to the laboratory reference system and can be computed from the azimuthal scattering intensity distribution according to[58]

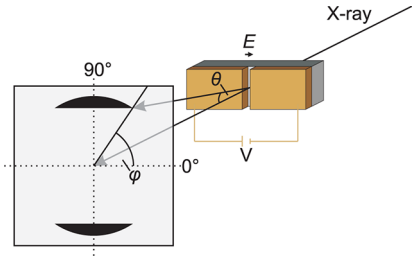

Figure 1. Setup for in situ SAXS experiments on polymer films in an in-plane electric field.

$$P_2 = \frac{3\langle\cos^2\varphi\rangle - 1}{2}$$

with

$$\langle\cos^2\varphi\rangle = \frac{\int_0^{2\pi} d\varphi(I_q(\varphi)\cos^2(\varphi)|\sin(\varphi)|)}{\int_0^{2\pi} d\varphi(I_q(\varphi)|\sin(\varphi)|)}$$

In the case of perfect lamellar orientation parallel to an applied electric field the scattering intensity distribution becomes anisotropic and accumulates at azimuthal angles $\phi = \pi/2$ and $\phi = 3\pi/2$ ($P_2 = -0.5$), while P_2 vanishes in the limit of an isotropic lamellar distribution ($P_2 = 0$).

Practically, $P_2 = -0.5$ is usually not reached: the electrodynamic driving force scales with the tilt angle φ between the lamellae normal and the electric field vector, with $\cos^2\varphi$ and, hence, becomes negligible for only slightly tilted interfaces respective to the field vector.[61] We also note that in the case of a weak signal in scattering experiments, background noise influences the absolute scattered intensity and, hence, the position of the first order Bragg peak q^*. Consequently, in order to assess the peak positions, especially at high q values, as precisely as possible, a baseline was subtracted that was automatically calculated from the intensity evolution at low q. Finally, q^* was determined by fitting the baseline-corrected radial intensity data using a Lorentz function. For the calculation of the orientational order parameter, the CCD images were background corrected by subtracting the detector background from the raw data.

We quantify the orientation kinetics by monitoring the time evolution of P_2 upon the inception of an electric field. In first approximation $P_2(t)$ follows pseudo-first-order kinetics according to

$$P_2(t) = P_{2,\infty} + (P_{2,0} - P_{2,\infty})e^{-t/\tau}$$

Here, τ denotes the time constant, and $P_{2,0}$ and $P_{2,\infty}$ are the lower and upper asymptotic limits for $t = 0$ and $t = \infty$. Thus, P_2 can be used not only for quantifying the quality of alignment, but also for investigating the kinetic behavior of block copolymers in electric fields.

We note that measurements not perpendicular to the surface but under an angle of 45° would reveal the orientation not only perpendicular to the film plane but also in the film's interior.[51,65,66] However, because of the constrained geometry with an electrode distance of only 40 μm, such measurements are not feasible. The needs of applying an electric field and measuring during solvent vapor annealing impose additional difficulties and require an X-ray exposure perpendicular to the substrate surface.

For our experiments, we used a nearly symmetric PS-*b*-P2VP block copolymer (54 vol % polystyrene (PS)) with a total number average molecular weight M_n = 99 kg/mol and a polydispersity M_w/M_n = 1.05.[67] We dispersed the polymer together with different amounts of spherical gold nanoparticles (Au-NP, diameter of 1.8 ± 0.6 nm, determined by TEM) with a dodecanethiol capping in toluene[68] and prepared films with a film thickness of approximately 3 ± 0.3 μm via drop-casting on custom designed electrode chips like shown in Figure 1. The chips consist of two planar evaporated gold electrodes on a 500 μm thick float glass substrate. The electrodes are separated by a 40 μm wide linear gap. By applying a voltage of 400 V, we generated a nearly homogeneous electric field of 10 V/μm.

After casting the films from toluene solutions, a micellar morphology was formed that transforms to lamellae during annealing.[67] Figure 2 shows SAXS CCD images during annealing the films for 60 min. Figure 2a and c show PS-*b*-P2VP films, neat and loaded with 3 wt % gold nanoparticles, respectively, which were annealed without the application of an electric field. The SAXS patterns indicate a randomly oriented, phase-separated structure with an average domain spacing D = 50.9 (a) and 52.6 nm (c). The nanoparticles are preferentially wetted by PS and are, thus, anticipated to accumulate primarily in the PS domains. We attribute the increase of lamellar periodicity in the presence of nanoparticles to the swelling PS domains, accordingly.[69] Figure 2b and d show similar films that

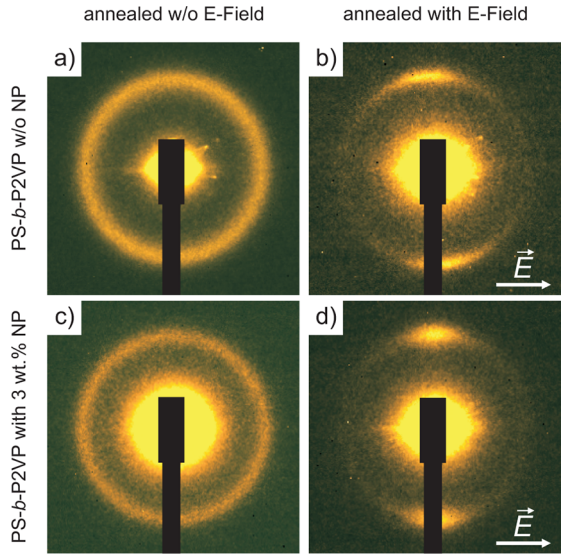

Figure 2. 2D SAXS patterns of PS-*b*-P2VP polymer films without (a, b) and with 3 wt % gold nanoparticles (c, d) during annealing in saturated toluene vapor for 60 min without (a, c) and with (b, d) simultaneously applied electric field of 10 V/μm.

dx.doi.org/10.1021/mz3005132 | ACS Macro Lett. 2013, 2, 53−58

were annealed under the application of an electric field. The peak scattering intensity accumulates at vertical azimuthal orientations indicating the parallel alignment of lamellae to the electric field vector (cf. Figure 1).

Figure 3 shows the film morphology of the samples from Figure 2 in the final dried state after annealing. AFM phase

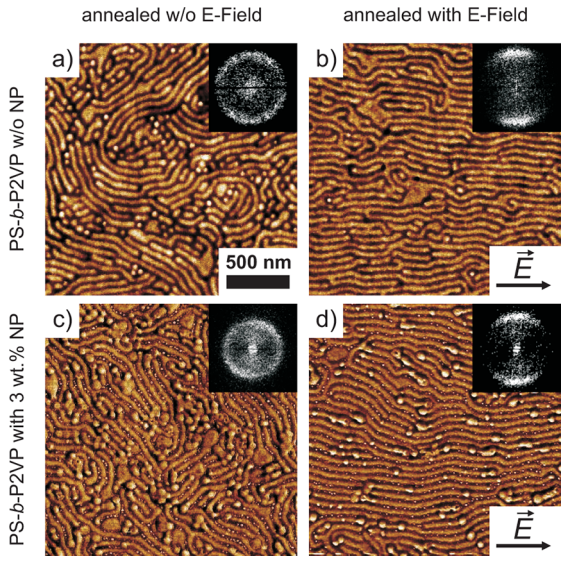

Figure 3. AFM phase images (phase contrast 10°) of PS-*b*-P2VP polymer films without (a, b) and with 3 wt % gold nanoparticles (c, d) after annealing in saturated toluene vapor without (a, c) and with (b, d) simultaneously applied electric field of 10 V/μm. The insets show Fourier transforms of the AFM images. Annealing times: 60 (a, c), 70 (b), and 90 min (d).

images show a nonoriented surface structure after annealing without electric field (Figure 3a,c). After application of an electric field, the striped structures have a preferential orientation in direction of the electric field (Figure 3b,d) as also evident from the insets that show Fourier transforms of the AFM images, representing the data from reciprocal space as could be recorded directly from SAXS. The scattering images, however, show the structural features of the same polymer films on a much larger scale as the X-ray beamsize exceeds the size of an AFM image by at least an order of magnitude. The morphology before annealing consists of micelles that break and slowly form lamellae during toluene vapor annealing.[67] Hence, the anisotropic structures in Figure 3 correspond to lamellae with remaining micelles (dot-like parts). The alignment still includes many defects, which may be a consequence of an insufficient field-strength, annealing time or entropic arguments as described above. The samples containing nanoparticles (Figure 3c,d) exhibit an increased number of micelle-defects. The AFM images were measured with moderate tapping conditions. Because the Young's moduli of PS and poly(2-vinyl pyridine) (P2VP) are 3.0 and 3.5 GPa, respectively,[70,71] the bright areas in AFM phase images can be assigned to the P2VP phase. The similarity of ex situ AFM and in situ SAXS data indicates that aligned structures do not lose the preferred orientation upon drying.

As is apparent from Figure 2, PS-*b*-P2VP containing 3 wt % nanoparticles (Figure 2d) is better aligned than without nanoparticles (Figure 2b). To quantify this behavior, we monitored the time evolution of P_2 as obtained from the scattering data upon inception of an electric field of 10 V/μm (Figure 4a). The order parameter decreases to approximately −0.20 with 3 wt % gold nanoparticles added to the film,

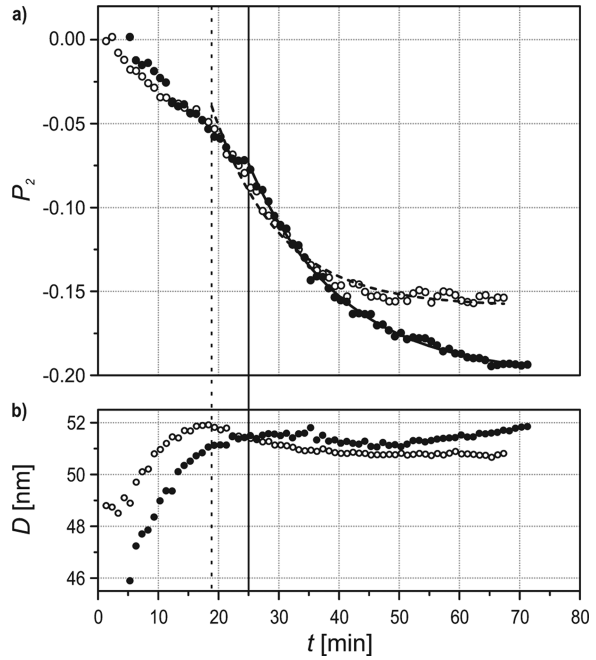

Figure 4. Order parameter P_2 (a) and average domain spacing D (b) as functions of experiment time for a pure PS-*b*-P2VP film (hollow circles) and for a composite film containing 3 wt % Au-NP in PS-*b*-P2VP (filled circles). The vertical lines mark the starting time of the exponential fit functions.

compared to a final P_2 of about −0.16 without nanoparticles. The individual data points deviate by less than 0.01. Hence, alignment with 3 wt % nanoparticles is significantly improved compared to the neat polymer film.

We can discriminate two regions in the $P_2(t)$ curve. In the early stages, P_2 follows a near-linear decline, while an exponential relaxation is evident at later stages. The behavior during the first minutes is attributed to film swelling. Olszowka et al. studied the swelling kinetics of a similar PS-*b*-P2VP diblock (50 wt % PS, M_n = 78 kg/mol). For annealing in saturated toluene vapor, the time until the film is swollen to its maximum extent is in the range of several minutes. If the vapor inside the annealing chamber is not saturated with solvent, the swelling time increases drastically.[27] For a longer PS-*b*-P2VP, Gensel et al. found that the thicker the polymer film, the longer it takes to reach the maximum swollen thickness. Even in a saturated atmosphere, this can be between tens of minutes to hours.[67] Because the swelling time is dependent on film thickness and vapor pressure, we expect the film to require tens of minutes to reach its fully swollen state. The initial micellar morphology that transforms to lamellae upon annealing is expected to additionally slow down swelling kinetics.

In Figure 4a, the attenuated orientation at the initial stages is well understood considering the reduced polymer chain mobility at low solvent concentration in the film. Both components of the block copolymer are glassy under ambient conditions and in the absence of solvent. Once the film becomes saturated with toluene during the course of solvent annealing, the applied field becomes the dominating factor influencing the alignment, which follows pseudo-first order kinetics, as reported previously.[61,62,64] The growth of the

dx.doi.org/10.1021/mz3005132 | *ACS Macro Lett.* 2013, 2, 53−58

lamellar periodicity D during solvent annealing is evident from a decrease in the radial location of the primary Bragg peak q^* according to $D = 2\pi/q^*$. Indeed, progressing solvent uptake in the initial stages leads to significant swelling of domains (cf. Figure 4b). In the late stages, D asymptotically converges to its equilibrium value determined by vapor pressure and the applied field strength at the given temperature. The decreasing D at longer experiment times suggests a denser packing of the polymer coils in the aligned polymer material.

With an increasing amount of Au-NP in the composite film, alignment takes significantly longer (Figure 5a). The

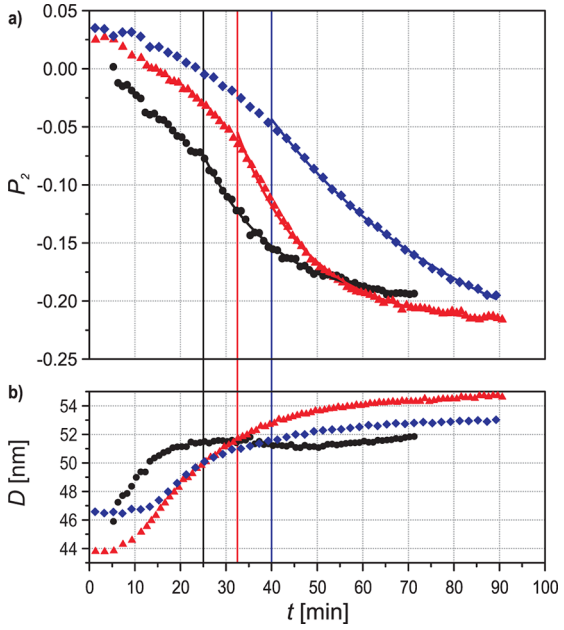

Figure 5. Order parameter P_2 (a) and average domain spacing D (b) as functions of experiment time for composite films containing 3 wt % (black circles), 6 wt % (red triangles), and 10 wt % (blue diamonds) Au-NP in PS-*b*-P2VP. The vertical lines mark the starting time of the exponential fit functions.

asymptotic orientational order parameters after several hours of E-field application ($P_{2,\infty}$) can be estimated from the fitting functions (exponential decay function $P_2(t) = P_{2,\infty} + A \cdot e^{-t/\tau}$), which are applied to swollen films. D shifts to higher values for the whole experiment time (experiments with 6 wt % and 10 wt % of gold nanoparticles, Figure 5b).

Figure 6 summarizes the asymptotic orientational order parameter $P_{2,\infty}$ and the time constant of composite alignment τ of the exponential fit functions with increasing nanoparticle concentration. For increasing nanoparticle fraction, $P_{2,\infty}$ decreases significantly. The errors in Figure 6 originate only from fitting. While the alignment improves with addition of nanoparticles to the block copolymer (lower $P_{2,\infty}$), the kinetics gets slower (higher τ). Furthermore, the initial swelling kinetics slows down as well with increasing nanoparticle loading.

The observed retardation of the electric-field induced alignment may be readily undestood in terms of increasing viscosity in the presence of nanoparticles.[72−74] More viscous block copolymer/nanoparticle composite materials may take longer to swell to the maximum degree due to a slower solvent uptake. Similarly, Chung and co-workers found the kinetics of phase separation in polymer blends to decrease with the addition of selective nanoparticles.[74] Additionally, by annealing,

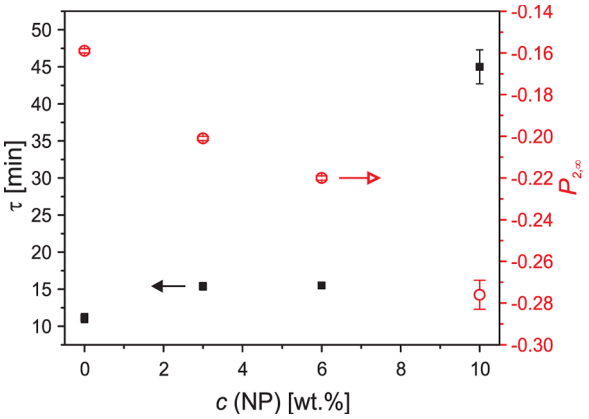

Figure 6. Time constants τ (black filled squares, left axis of ordinates) and asymptotic orientational order parameter $P_{2,\infty}$ (red hollow circles, right axis of ordinates) of the exponential fit functions displayed in Figures 4 and 5 (PS-*b*-P2VP with Au-NP like indicated).

nanoparticle distribution in the block copolymer domains improves, and the domain size slowly approaches the equilibrium state. This takes longer for higher the nanoparticle loading. Hence, the annealing time before an exponential decay fit increases with nanoparticle content. The alignment in an electric field is similarly influenced and takes longer for more viscous systems, i.e., those containing more nanoparticles.

As the swelling may not yet be completed in the time range before the exponential fit is applied, the pure alignment kinetics without other influences is potentially faster than indicated. We therefore regard the time constants solely as a relative measure, which affords a qualitative comparison of the alignment kinetics in the absence and presence of nanoparticles and do not attempt any quantitative interpretation.

The decreasing $P_{2,\infty}$ indicates an improved order in the composite films with addition of nanoparticles. Selective addition of nanoparticles to one phase of a diblock is expected to significantly increase the dielectric contrast.[39,40] Further, nanoparticles enhance undulations of the lamellar thickness that serve as nuclei for alignment.[75−77] The reduction of $P_{2,\infty}$ can thus be explained as enhanced effect of the electric field on the nanocomposite caused by nanoparticle-induced increase in dielectric contrast and destabilized interfaces.

In this contribution, we investigated the influence nanoparticles have on the kinetics of block copolymer alignment under an applied electric field. By adding selective gold nanoparticles to a PS-*b*-P2VP film, application of an electric field leads to improved order compared to the neat polymer film. Indeed, with increasing nanoparticle fraction (in the range 3−10 wt % nanoparticles), the alignment improves with increasing amounts of added nanoparticles. However, it takes significantly longer to reach the final aligned structure. Furthermore, our experiments indicate a slower swelling kinetics. We explained the better alignment with the increased dielectric contrast in composites with a high nanoparticle fraction and, hence, a higher susceptibility for electric fields. The slower kinetics results from the increasing viscosity by addition of nanoparticles.

■ ASSOCIATED CONTENT

Supporting Information

Experimental details. This material is available free of charge via the Internet at http://pubs.acs.org.

dx.doi.org/10.1021/mz3005132 | *ACS Macro Lett.* 2013, 2, 53−58

AUTHOR INFORMATION

Corresponding Author

*E-mail: boeker@dwi.rwth-aachen.de. Phone: +49 (0)241 8023304. Fax: +49 (0)241 8023317.

Notes

The authors declare no competing financial interest.

ACKNOWLEDGMENTS

Our scattering experiments were performed on the ID2 beamline at the European Synchrotron Radiation Facility (ESRF), Grenoble, France. We thank Klaus Kreuels and Zhirong Fan for assistance, Theyencheri Narayanan for affording additional beam time, and we are grateful to the ESRF for financial support and provision of synchrotron beam time. C.L., C.W.P., M.J.P., R.S., and A.B. thank the European Union and the German Science Foundation (DFG, BO 2475/5-1) for financial support in the framework of the ERA-NanoSci-E+ project MEMORY. M.R. and V.S.U. were supported by the U.S. Department of Energy, Office of Science, Basic Energy Science, Materials Science and Engineering Division.

REFERENCES

(1) Matsen, M. W.; Bates, F. S. *Macromolecules* **1996**, *29*, 1091−1098.
(2) Ciebien, J. F.; Clay, R. T.; Sohn, B. H.; Cohen, R. E. *New J. Chem.* **1998**, *22*, 685−691.
(3) Sohn, B. H.; Seo, B. W.; Yoo, S. I. *J. Mater. Chem.* **2002**, *12*, 1730−1734.
(4) Keller, A.; Pedemonte, E.; Willmouth, F. M. *Nature* **1970**, *225*, 538−539.
(5) Albalak, R. J.; Thomas, E. L. *J. Polym. Sci., Part B: Polym. Phys.* **1993**, *31*, 37−46.
(6) Wiesner, U. *Macromol. Chem. Phys.* **1997**, *198*, 3319−3352.
(7) Chen, Z.-R.; Kornfield, J. A.; Smith, S. D.; Grothaus, J. T.; Satkowski, M. M. *Science* **1997**, *277*, 1248−1253.
(8) Angelescu, D. E.; Waller, J. H.; Register, R. A.; Chaikin, P. M. *Adv. Mater.* **2005**, *17*, 1878−1881.
(9) Kim, S. H.; Misner, M. J.; Xu, T.; Kimura, M.; Russell, T. P. *Adv. Mater.* **2004**, *16*, 226−231.
(10) Yoon, J.; Lee, W.; Thomas, E. L. *Adv. Mater.* **2006**, *18*, 2691−2694.
(11) Hashimoto, T.; Bodycomb, J.; Funaki, Y.; Kimishima, K. *Macromolecules* **1999**, *32*, 952−954.
(12) Segalman, R. A.; Yokoyama, H.; Kramer, E. J. *Adv. Mater.* **2001**, *13*, 1152−1155.
(13) Cheng, J. Y.; Ross, C. A.; Smith, H. I.; Thomas, E. L. *Adv. Mater.* **2006**, *18*, 2505−2521.
(14) Ruiz, R.; Kang, H.; Detcheverry, F. A.; Dobisz, E.; Kercher, D. S.; Albrecht, T. R.; de Pablo, J. J.; Nealey, P. F. *Science* **2008**, *321*, 936−939.
(15) Galatsis, K.; Wang, K. L.; Ozkan, M.; Ozkan, C. S.; Huang, Y.; Chang, J. P.; Monbouquette, H. G.; Chen, Y.; Nealey, P.; Botros, Y. *Adv. Mater.* **2010**, *22*, 769−778.
(16) Hamley, I. W.; Castelletto, V.; Lu, Z. B.; Imrie, C. T.; Itoh, T.; Al-Hussein, M. *Macromolecules* **2004**, *37*, 4798−4807.
(17) Tao, Y.; Zohar, H.; Olsen, B. D.; Segalman, R. A. *Nano Lett.* **2007**, *7*, 2742−2746.
(18) Gopinadhan, M.; Majewski, P. W.; Osuji, C. O. *Macromolecules* **2010**, *43*, 3286−3293.
(19) Majewski, P. W.; Gopinadhan, M.; Osuji, C. O. *J. Polym. Sci., Part B: Polym. Phys.* **2012**, *50*, 2−8.
(20) Gopinadhan, M.; Majewski, P. W.; Beach, E. S.; Osuji, C. O. *ACS Macro Lett.* **2012**, *1*, 184−189.
(21) Amundson, K.; Helfand, E.; Davis, D. D.; Quan, X.; Patel, S. S.; Smith, S. D. *Macromolecules* **1991**, *24*, 6546−6548.
(22) Morkved, T. L.; Lu, M.; Urbas, A. M.; Ehrichs, E. E.; Jaeger, H. M.; Mansky, P.; Russell, T. P. *Science* **1996**, *273*, 931−933.
(23) Xu, T.; Zhu, Y. Q.; Gido, S. P.; Russell, T. P. *Macromolecules* **2004**, *37*, 2625−2629.
(24) Xu, T.; Zvelindovsky, A. V.; Sevink, G. J. A.; Lyakhova, K. S.; Jinnai, H.; Russell, T. P. *Macromolecules* **2005**, *38*, 10788−10798.
(25) Olszowka, V.; Hund, M.; Kuntermann, V.; Scherdel, S.; Tsarkova, L.; Böker, A.; Krausch, G. *Soft Matter* **2006**, *2*, 1089−1094.
(26) Olszowka, V.; Hund, M.; Kuntermann, V.; Scherdel, S.; Tsarkova, L.; Böker, A. *ACS Nano* **2009**, *3*, 1091−1096.
(27) Olszowka, V.; Tsarkova, L.; Böker, A. *Soft Matter* **2009**, *5*, 812−819.
(28) Liedel, C.; Hund, M.; Olszowka, V.; Böker, A. *Soft Matter* **2012**, *8*, 995−1002.
(29) Liedel, C.; Pester, C. W.; Ruppel, M.; Urban, V. S.; Böker, A. *Macromol. Chem. Phys.* **2012**, *213*, 259−269.
(30) Tsutsumi, K.; Funaki, Y.; Hirokawa, Y.; Hashimoto, T. *Langmuir* **1999**, *15*, 5200−5203.
(31) Sohn, B.-H.; Choi, J.-M.; Yoo, S. I.; Yun, S.-H.; Zin, W.-C.; Jung, J. C.; Kanehara, M.; Hirata, T.; Teranishi, T. *J. Am. Chem. Soc.* **2003**, *125*, 6368−6369.
(32) Chiu, J. J.; Kim, B. J.; Kramer, E. J.; Pine, D. J. *J. Am. Chem. Soc.* **2005**, *127*, 5036−5037.
(33) Minelli, C.; Hinderling, C.; Heinzelmann, H.; Pugin, R.; Liley, M. *Langmuir* **2005**, *21*, 7080−7082.
(34) Shenhar, R.; Jeoung, E.; Srivastava, S.; Norsten, T. B.; Rotello, V. M. *Adv. Mater.* **2005**, *17*, 2206−2210.
(35) Balazs, A. C.; Emrick, T.; Russell, T. P. *Science* **2006**, *314*, 1107−1110.
(36) Pavan, M. J.; Shenhar, R. *J. Mater. Chem.* **2011**, *21*, 2028−2040.
(37) Chung, H.-J.; Kim, J.; Ohno, K.; Composto, R. J. *ACS Macro Lett.* **2012**, *1*, 252−256.
(38) Bockstaller, M. R.; Mickiewicz, R. A.; Thomas, E. L. *Adv. Mater.* **2005**, *17*, 1331−1349.
(39) Schürmann, U.; Takele, H.; Zaporojtchenko, V.; Faupel, F. *Thin Solid Films* **2006**, *515*, 801−804.
(40) Ginzburg, V. V.; Myers, K.; Malowinski, S.; Cieslinski, R.; Elwell, M.; Bernius, M. *Macromolecules* **2006**, *39*, 3901−3906.
(41) Peponi, L.; Tercjak, A.; Gutierrez, J.; Stadler, H.; Torre, L.; Kenny, J. M.; Mondragon, I. *Macromol. Mater. Eng.* **2008**, *293*, 568−573.
(42) Yan, L.-T.; Schoberth, H. G.; Böker, A. *Soft Matter* **2010**, *6*, 5956−5964.
(43) Melde, B. J.; Burkett, S. L.; Xu, T.; Goldbach, J. T.; Russell, T. P.; Hawker, C. J. *Chem. Mater.* **2005**, *17*, 4743−4749.
(44) Hillmyer, M. A. *Adv. Polym. Sci.* **2005**, *190*, 137−181.
(45) Olson, D. A.; Chen, L.; Hillmyer, M. A. *Chem. Mater.* **2008**, *20*, 869−890.
(46) Förster, S.; Antonietti, M. *Adv. Mater.* **1998**, *10*, 195−217.
(47) Chai, J.; Wang, D.; Fan, X.; Buriak, J. M. *Nat. Nanotechnol.* **2007**, *2*, 500−506.
(48) Chai, J.; Buriak, J. M. *ACS Nano* **2008**, *2*, 489−501.
(49) Mansky, P.; DeRouchey, J.; Russell, T. P.; Mays, J.; Pitsikalis, M.; Morkved, T.; Jaeger, H. *Macromolecules* **1998**, *31*, 4399−4401.
(50) Thurn-Albrecht, T.; Steiner, R.; DeRouchey, J.; Stafford, C. M.; Huang, E.; Bal, M.; Tuominen, M.; Hawker, C. J.; Russell, T. *Adv. Mater.* **2000**, *12*, 787−791.
(51) Thurn-Albrecht, T.; DeRouchey, J.; Russell, T. P.; Jaeger, H. M. *Macromolecules* **2000**, *33*, 3250−3253.
(52) Böker, A.; Knoll, A.; Elbs, H.; Abetz, V.; Müller, A. H. E.; Krausch, G. *Macromolecules* **2002**, *35*, 1319−1325.
(53) Thurn-Albrecht, T.; DeRouchey, J.; Russell, T. P.; Kolb, R. *Macromolecules* **2002**, *35*, 8106−8110.
(54) Xu, T.; Hawker, C. J.; Russell, T. P. *Macromolecules* **2003**, *36*, 6178−6182.
(55) Xu, T.; Goldbach, J. T.; Russell, T. P. *Macromolecules* **2003**, *36*, 7296−7300.
(56) DeRouchey, J.; Thurn-Albrecht, T.; Russell, T. P.; Kolb, R. *Macromolecules* **2004**, *37*, 2538−2543.

(57) Wang, J. Y.; Leiston-Belanger, J. M.; Sievert, J. D.; Russell, T. P. *Macromolecules* **2006**, *39*, 8487−8491.
(58) Amundson, K.; Helfand, E.; Quan, X.; Smith, S. D. *Macromolecules* **1993**, *26*, 2698−2703.
(59) Amundson, K.; Helfand, E.; Quan, X.; Hudson, S. D.; Smith, S. D. *Macromolecules* **1994**, *27*, 6559−6570.
(60) Böker, A.; Hänsel, H.; Elbs, H.; Knoll, A.; Ludwigs, S.; Zettl, H.; Urban, V.; Abetz, V.; Müller, A. H. E.; Krausch, G. *Phys. Rev. Lett.* **2002**, *89*, 135502.
(61) Böker, A.; Elbs, H.; Hänsel, H.; Knoll, A.; Ludwigs, S.; Zettl, H.; Zvelindovsky, A. V.; Sevink, G. J. A.; Urban, V.; Abetz, V.; Müller, A. H. E.; Krausch, G. *Macromolecules* **2003**, *36*, 8078−8087.
(62) Schmidt, K.; Böker, A.; Zettl, H.; Schubert, F.; Hänsel, H.; Fischer, F.; Weiss, T. M.; Abetz, V.; Zvelindovsky, A. V.; Sevink, G. J. A.; Krausch, G. *Langmuir* **2005**, *21*, 11974−11980.
(63) Böker, A.; Schmidt, K.; Knoll, A.; Zettl, H.; Hänsel, H.; Urban, V.; Abetz, V.; Krausch, G. *Polymer* **2006**, *47*, 849−857.
(64) Schmidt, K.; Schoberth, H. G.; Schubert, F.; Hänsel, H.; Fischer, F.; Weiss, T. M.; Sevink, G. J. A.; Zvelindovsky, A. V.; Böker, A.; Krausch, G. *Soft Matter* **2007**, *3*, 448−453.
(65) Jung, Y.; Cho, T.-Y.; Yoon, D. Y.; Frank, C. W.; Luüning, J. *Macromolecules* **2005**, *38*, 867−872.
(66) Pattison, L. R.; Hexemer, A.; Kramer, E. J.; Krishnan, S.; Petroff, P. M.; Fischer, D. A. *Macromolecules* **2006**, *39*, 2225−2231.
(67) Gensel, J.; Liedel, C.; Schoberth, H. G.; Tsarkova, L. *Soft Matter* **2009**, *5*, 2534−2537.
(68) Brust, M.; Walker, M.; Bethell, D.; Schiffrin, D. J.; Whyman, R. *J. Chem. Soc., Chem. Commun.* **1994**, *7*, 801−802.
(69) Sides, S. W.; Kim, B. J.; Kramer, E. J.; Fredrickson, G. H. *Phys. Rev. Lett.* **2006**, *96*, 250601.
(70) Xu, T.; Goldbach, J. T.; Misner, M. J.; Kim, S.; Gibaud, A.; Gang, O.; Ocko, B.; Guarini, K. W.; Black, C. T.; Hawker, C. J.; Russell, T. P. *Macromolecules* **2004**, *37*, 2972−2977.
(71) Lee, J.-Y.; Crosby, A. Combinatorial Investigation of Crazes in Polymer Nanocomposites; APS March Meeting, Los Angeles, CA, March 21−25, 2005, American Physical Society: College Park, MD, 2005; abstract C1.155.
(72) Krishnamoorti, R.; Ren, J.; Silva, A. S. *J. Chem. Phys.* **2001**, *114*, 4968−4973.
(73) Steinmann, S.; Gronski, W.; Friedrich, C. *Polymer* **2002**, *43*, 4467−4477.
(74) Chung, H.-J.; Taubert, A.; Deshmukh, R. D.; Composto, R. J. *Europhys. Lett.* **2004**, *68*, 219−225.
(75) Onuki, A.; Fukuda, J.-I. *Macromolecules* **1995**, *28*, 8788−8795.
(76) Fukuda, J.-I.; Onuki, A. *J. Phys. II (France)* **1995**, *5*, 1107−1113.
(77) Matsen, M. W. *Soft Matter* **2006**, *2*, 1048−1056.